Materials Research. 2026; 29: e20260021
DOI: https://doi.org/10.1590/1980-5373-MR-2026-0021

Discrete Microstructural Pathway Modeling of Recrystallization Using Three-Dimensional Hybrid Cellular Automata

***Henrique Costa Braga*[a]*, *Sidney Nicodemos da Silva*[b], *Elaine Carballo Siqueira Corrêa*[b]**

[a]*Centro Federal de Educação Tecnológica de Minas Gerais (CEFET-MG), Departamento de Engenharia de Transportes, Belo Horizonte, MG, Brasil.*
[b]*Centro Federal de Educação Tecnológica de Minas Gerais (CEFET-MG), Programa de Pós-Graduação em Engenharia de Materiais, Belo Horizonte, MG, Brasil.*

Received: January 21, 2026; Revised: April 19, 2026; Accepted: May 18, 2026

The quantitative analysis of recrystallization microstructures requires methodologies capable of describing interfacial evolution clearly and with minimal reliance on phenomenological assumptions. Although microstructural paths relating interfacial surface area density to transformed volume fraction are well-established in experimental and hybrid modeling studies, their determination commonly depends on analytical kinetic formulations or fitted parameters. In this work, a fully discrete formulation of the recrystallization microstructural path is proposed based on three-dimensional hybrid cellular automata simulations. All relevant descriptors, including the transformed volume fraction and the interfacial surface area density between recrystallized and non-recrystallized regions, are obtained directly from voxel-level geometric information, without invoking phenomenological kinetic equations or auxiliary correction factors. The methodology is applied to different growth geometries, encompassing classical face-based cellular automata growth as well as spherical and spheroidal grain growth within a hybrid framework. The resulting microstructural paths reproduce the characteristic non-monotonic behavior reported in experimental and computational studies in the literature. Comparative analyses show that grain morphology significantly influences microstructural path evolution, highlighting the importance of geometric assumptions in recrystallization modeling. The proposed approach provides a transparent and reproducible framework for analyzing recrystallization microstructures and offers an independent, geometry-based perspective that complements traditional kinetic descriptions.

Keywords: *Recrystallization, Microstructural path, Hybrid cellular automata, Interfacial surface area density, Computational microstructure.*

1. Introduction

Recrystallization plays a central role in the restoration of ductility and in the evolution of grain structure in plastically deformed metals, directly influencing mechanical strength, anisotropy, texture development, and formability. Owing to its relevance in thermomechanical processing routes, extensive experimental and theoretical efforts have been devoted to the description of recrystallization kinetics and microstructural evolution[1-3].

Traditionally, recrystallization kinetics have been described using phenomenological formulations, most notably Kolmogorov–Johnson–Mehl–Avrami (KJMA) type models, which provided an early framework for kinetic analysis based on simplified geometric and statistical assumptions[3-6]. These approaches necessarily incorporate idealizations regarding nucleation behavior, growth geometry, and spatial homogeneity, reflecting the balance between physical realism and analytical tractability inherent to continuum-based kinetic modeling. Within this context, the concept of the microstructural path was introduced, describing recrystallization through the coupled evolution of transformed volume fraction and interfacial surface area density, thereby shifting the focus from purely kinetic descriptions toward microstructure-based representations of transformation kinetics[1,3,7].

In parallel with experimental developments, computational modeling has emerged as a powerful tool for investigating recrystallization mechanisms beyond analytical constraints. Among the various numerical approaches available, cellular automata (CA) models were among the earliest fully computational techniques extensively applied to recrystallization phenomena[8-11]. Their widespread adoption is largely attributed to their discrete formulation, relatively low computational cost, and ability to explicitly represent key microstructural mechanisms such as nucleation, grain growth, and impingement in both two- and three-dimensional domains[12-14]. As a result, CA-based models have played a foundational role in mesoscale recrystallization modeling and have served as a reference framework for subsequent methodological developments.

However, the discrete lattice and neighborhood definitions inherent to conventional CA schemes introduce geometric

*email: henriquebraga@cefetmg.br
Associate Editor: Hugo Sandim.
Editor-in-Chief: Luiz Antonio Pessan.

constraints that influence grain morphology and interface topology. In particular, the resulting anisotropy is not a physical attribute intentionally introduced to represent material behavior, but rather a numerical artifact associated with lattice geometry and neighbor selection. This effect is inherent to classical CA formulations and persists throughout the recrystallization process due to discretization-induced geometric constraints[8]. It is, however, more readily observed during the early stages of grain growth, prior to impingement, when grain shapes are more clearly defined[5].

The geometric anisotropy inherent to conventional cellular automata formulations has motivated the development of several strategies aimed at improving grain-shape representation and interfacial fidelity in recrystallization modeling[8,12]. These strategies include the use of extended or weighted neighborhoods, probabilistic transition rules, lattice reorientation schemes, and coupling with continuous geometric descriptions.

Within this context, hybrid cellular automata (HCA) approaches have been proposed as an extension of classical CA models, in which the microstructure remains discretely represented on a voxel lattice while grain growth is governed by continuous geometric rules. By decoupling grain-shape evolution from lattice topology, this formulation enables improved geometric fidelity and allows the generation of various geometries, including equiaxed, spherical, or spheroidal grains, without compromising the computational efficiency and local update characteristics inherent to discrete automata. Recent studies have demonstrated that HCA-based models provide an enhanced description of grain morphology and interfacial evolution when compared to conventional CA schemes[15,16]. These findings are consistent with broader discussions in the literature emphasizing the importance of adequately capturing structural variability for physically meaningful materials modeling[12,17].

In the existing literature, the modeling of recrystallization kinetics and microstructural path evolution is commonly conducted using mixed or hybrid strategies, in which discrete computational simulations are combined with phenomenological formulations derived from experimental observations. In this context, computational models are frequently employed to represent nucleation, growth, and impingement processes, while analytical expressions, most notably those associated with the KJMA framework or related geometric formulations, are used to guide, interpret, or parameterize the evolution of transformed volume fraction and interfacial surface area density.

Within microstructural path modeling, several seminal and subsequent studies have explicitly adopted this mixed approach. Rios and Padilha[1] and Vandermeer[3] further developed the microstructural path concept by relating transformed volume fraction and interfacial surface density through analytical expressions grounded in idealized geometric assumptions. These formulations have provided a powerful interpretative framework and remain used as reference models for recrystallization kinetics.

Later developments incorporated computational simulations to complement these analytical descriptions. For instance, Salazar et al.[18] employed cellular automata simulations to generate evolving microstructures, while relying on phenomenological relations to construct and interpret the corresponding microstructural paths. Similar mixed strategies have been adopted in subsequent studies, in which discrete simulations and analytical kinetic or geometric descriptions are used in conjunction to interpret microstructural evolution[7,10,19], often grounded in classical nucleation-and-growth formulations such as those described in[20].

A related perspective is found in quantitative metallography studies, such as that of Alves et al.[21], where microstructural descriptors are rigorously defined and measured, and their relationship to transformation kinetics is systematically analyzed. Although these approaches provide valuable and physically meaningful descriptors, they do not explicitly aim to construct microstructural paths exclusively from discrete geometric information.

In this sense, the use of hybrid computational and phenomenological formulations represents not a limitation, but rather a deliberate and widely adopted modeling practice. Nevertheless, a formulation capable of determining microstructural paths directly from evolving digital microstructures, without invoking phenomenological kinetic equations or auxiliary fitting parameters, offers an alternative perspective. Such a fully discrete approach enables the simultaneous tracking of transformed volume fraction and interfacial surface area density based solely on voxel-level geometric information, providing a self-consistent, geometry-based description of recrystallization kinetics.

In this context, the present work introduces a fully discrete description of the microstructural pathway of recrystallization based on three-dimensional hybrid cellular automata. The proposed methodology enables the direct computation of both the transformed volume fraction and the interfacial surface area density from the voxelized microstructure throughout the simulation, without resorting to analytical kinetic laws such as KJMA or auxiliary fitting parameters. By systematically comparing different grain growth geometries, including classical CA-based growth and HCA-based spheroidal growth, the influence of grain morphology on microstructural path evolution is examined. The resulting framework offers a physically consistent and computationally robust alternative for the analysis of recrystallization kinetics in metallic materials.

2. Methodology

2.1. Computational framework

The proposed methodology is based on three-dimensional hybrid cellular automata (HCA), in which the microstructure is discretized into a regular voxel lattice while grain growth is governed by continuous geometric constraints. Each voxel represents a volume element of the material and is assigned either to a recrystallized grain or to the non-recrystallized matrix. Grain nuclei are randomly distributed within the computational domain at the initial simulation step, with the nucleation density prescribed as an input parameter.

Grain growth proceeds through the progressive occupation of neighboring voxels according to deterministic geometric rules defined at the grain level. Unlike stochastic cellular automata formulations, no probabilistic switching criteria are employed. The simulation evolves as grains expand and

impinge upon one another until the computational domain becomes fully recrystallized.

All visualizations and geometric interpretations adopt the standard Cartesian coordinate convention, consistent with the representation illustrated in[15].

2.2. Grain growth geometries

Two growth regimes are considered for comparative analysis. In the classical CA formulation, grain growth follows an octahedral geometry imposed by the face-based neighborhood structure of the cubic lattice, resulting in faceted grains and pronounced lattice-induced anisotropy. This formulation is representative of conventional CA-based recrystallization models.

In contrast, the HCA formulation enforces continuous geometric constraints that allow grains to grow as spheres or spheroids within the voxelized domain. In this case, grain morphology is decoupled from lattice topology and controlled explicitly through geometric parameters.

Grain shape in the HCA framework is defined by the axial ratio K_a, corresponding to the ratio between the principal growth axes. Equiaxed growth is obtained for $K_a = 1$, whereas prolate and oblate spheroidal morphologies correspond to $K_a > 1$ and $K_a < 1$, respectively[16]. This parameterization enables a systematic investigation of the influence of growth anisotropy on recrystallization kinetics and microstructural path evolution.

2.3. Discrete representation of recrystallization

Recrystallization is modeled as a fully discrete phase transformation from a non-recrystallized to a recrystallized state. No explicit stored-energy fields, recovery kinetics, or phenomenological rate equations are introduced. Instead, the transformation progresses exclusively through deterministic grain growth and impingement processes.

At each simulation step, voxels are classified according to their state, providing direct access to the evolving topology of the microstructure. This discrete representation enables the explicit identification of interfaces between recrystallized and non-recrystallized regions throughout the transformation.

Interfacial surface area is computed directly from the voxelized microstructure by counting face-adjacent voxel pairs in different states, an approach aligned with general methodologies for geometric characterization of discretized microstructures and digital materials analysis[22-25]. Both the transformed volume fraction and the interfacial surface area density therefore emerge as intrinsic outputs of the simulation, without the need for auxiliary analytical formulations.

2.4. Computation of the microstructural path

The microstructural path is defined as the coupled evolution of transformed volume fraction and interfacial surface area density during recrystallization. The transformed volume fraction is calculated as the ratio between the number of recrystallized voxels and the total number of voxels in the computational domain.

The interfacial surface area density is obtained by normalizing the total interfacial area between recrystallized and non-recrystallized regions by the simulation volume. By tracking these quantities throughout the simulation, a fully discrete microstructural path curve is constructed.

This approach provides a direct geometric description of recrystallization kinetics, in contrast to conventional methods based on fitting transformed fraction data to analytical expressions such as the KJMA equation.

2.5. Simulation conditions and post-processing

All simulations are performed on cubic domains with identical lattice resolution and nucleation density to ensure direct comparability between different growth geometries. To minimize boundary effects, interfacial contributions associated with the domain boundaries are excluded from the surface area calculations. In particular, only interfaces between recrystallized and non-recrystallized regions within the interior of the domain are considered, while contacts between grains and the external domain surfaces are not included. This procedure ensures that the computed geometric descriptors are not affected by truncation artifacts at the domain limits.

The resulting microstructural path curves are compared across different growth regimes, highlighting the influence of grain morphology and growth anisotropy on the evolution of transformed volume fraction and interfacial surface area density. Experimental microstructural path data reported in the literature are used for qualitative validation of the proposed discrete framework.

3. Results and Discussion

3.1. Classical microstructural path concept and interfacial descriptors

During recrystallization, newly formed grains generate two distinct types of external interfaces. At the early stages of the process, the dominant interfaces are those formed between recrystallized regions and the surrounding non-recrystallized microstructure. As recrystallization progresses and growing grains begin to impinge on one another, a second type of interface emerges, corresponding to boundaries formed between adjacent recrystallized grains. With continued transformation, the relative contribution of recrystallized–recrystallized interfaces increases, while interfaces with the original microstructure progressively vanish. Upon completion of recrystallization, only interfaces between recrystallized grains remain.

To quantitatively describe microstructural evolution during recrystallization, two interfacial surface area densities are defined. The interfacial surface area density between recrystallized and non-recrystallized regions is denoted by S_{VRN}, whereas the interfacial surface area density between two recrystallized regions is denoted by S_{VRR}. These descriptors provide a direct geometric characterization of the evolving microstructure. Although both descriptors are relevant for a complete description of the evolving interface network, the present work focuses on S_{VRN}, which directly characterizes the interface between recrystallized and non-recrystallized regions during transformation.

Under the assumptions of random grain distribution and site-saturated nucleation, classical stereological analysis relates the extended interfacial surface area density, S_{Vex}, to S_{VRN}, as a function of the transformed volume fraction, X_r [1,26]:

$$S_{Vex} = \frac{S_{VRN}}{1 - X_r} \tag{1}$$

Assuming spherical grain geometry in extended space, the surface area of an individual grain, S_e, is given by:

$$S_e = 4\pi R_{ex}^2 \tag{2}$$

where R_{ex} is the extended grain radius. For a population of N_V recrystallized grains per unit volume, the extended interfacial surface area density is expressed as:

$$S_{Vex} = 4\pi R_{ex}^2 N_V \tag{3}$$

Considering the volume of spherical grains in extended space, the extended transformed volume fraction, X_{ex}, is defined as:

$$X_{ex} = \left(\frac{4}{3}\pi R_{ex}^3 N_V\right) \tag{4}$$

By eliminating R_{ex} between Eqs. (3) and (4), a direct relationship between S_{Vex} and X_{ex} is obtained. Combining this result with the exact relationship between X_{ex} and X_r derived from classical transformation kinetics, which can be expressed in differential form as $dX_r / dX_{ex} = 1 - X_r$ [7] and, upon integration, yields:

$$X_{ex} = ln\left(\frac{1}{1 - X_r}\right) \tag{5}$$

leads to an expression relating S_{Vex} and X_r. Using Equation (1) to express S_{Vex} in terms of S_{VRN}, the resulting expression can be rewritten as a function of S_{VRN} and X_r, yielding the classical microstructural path equation for site-saturated nucleation and random grain distribution, given by[1,26]:

$$S_{VRN} = 3\left(\frac{4\pi N_V}{3}\right)^{1/3}(1 - X_r)\left[ln\left(\frac{1}{1 - X_r}\right)\right]^{2/3} \tag{6}$$

Equation (6) defines the classical microstructural path of recrystallization, relating the interfacial surface area density between recrystallized and non-recrystallized regions, S_{VRN}, to the transformed volume fraction X_r. This formulation has been extensively used in geometrical and stereological analyses to describe recrystallization kinetics and microstructural evolution under assumptions of random nucleation and isotropic growth[1,26,27].

Figure 1 schematically illustrates a typical microstructural-path curve, in which S_{VRN} initially increases from zero, reaches a maximum at intermediate transformation stages, and subsequently decreases back to zero as recrystallization approaches completion. This behavior reflects the underlying microstructural mechanisms: at early stages, the total interfacial area increases due to the growth of isolated recrystallized grains within the original matrix; as grain impingement becomes significant, growth is progressively constrained, leading to a maximum in S_{VRN}; finally, the disappearance of interfaces with the non-recrystallized matrix causes S_{VRN} to decrease, vanishing once recrystallization is complete.

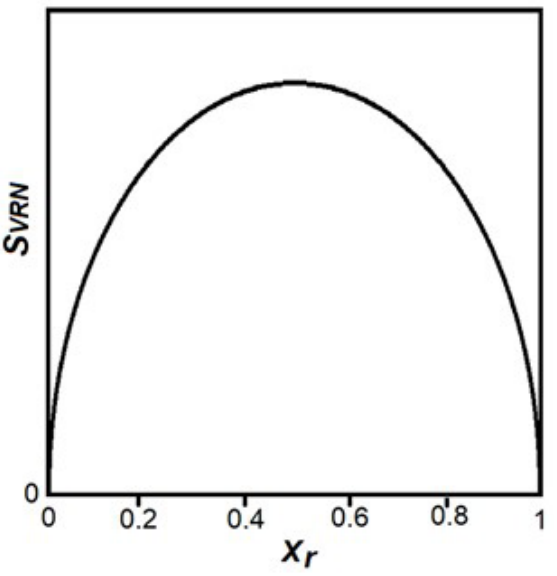

Figure 1. Schematic microstructural path (S_{VRN} versus X_r).

3.2. From hybrid to fully discrete microstructural path modeling

The classical microstructural path formulation relates S_{VRN} to the transformed volume fraction, X_r, through analytical expressions derived under specific assumptions regarding nucleation and growth conditions. As discussed in Section 3.1, this relationship has been widely employed to analyze recrystallization kinetics and is often discussed alongside phenomenological kinetic descriptions (e.g., KJMA-type analyses).

Within a computational framework, X_r is directly obtained from the simulation by evaluating the fraction of the domain occupied by recrystallized voxels. Here, τ denotes the discrete simulation step (iteration index). Denoting by $N_{CT}(\tau)$ the number of transformed cells at simulation step τ and by C_n the total number of cells in the simulation domain, the transformed volume fraction is given by:

$$X_r(\tau) = \frac{N_{CT}(\tau)}{C_n} \tag{7}$$

Substituting Equation (7) into the analytical microstructural path expression allows the construction of $S_{VRN} - X_r$ curves using simulation-derived data combined with phenomenological equations. This procedure constitutes a hybrid approach, in which discrete simulation outputs are coupled with analytical formulations originally derived from continuous, experimental considerations.

Although valid from a theoretical standpoint, the hybrid formulation presents intrinsic limitations. While it enables the estimation of selected microstructural descriptors, it does not exploit the full amount of geometric information available in voxel-based simulations. Moreover, by relying on predefined analytical expressions, the hybrid approach may partially constrain the resulting microstructural path

curves toward expected phenomenological trends, potentially obscuring deviations arising from specific growth geometries or interface topologies.

In contrast, the fully discrete nature of the present simulations provides direct access to all voxels constituting the evolving microstructure. This allows both the transformed volume fraction X_r and the interfacial surface area density S_{VRN} to be computed intrinsically, without invoking analytical expressions or phenomenological correction factors. In this fully discrete formulation, interfacial areas are obtained directly from the voxelized microstructure by identifying and counting face-adjacent voxel pairs belonging to different transformation states.

Accordingly, the microstructural path can be constructed exclusively from discrete geometric information, reflecting the actual morphology and topology of the simulated microstructure. This approach eliminates dependence on phenomenological kinetics, such as Avrami or KJMA formulations, and enables an unbiased assessment of recrystallization behavior driven solely by the underlying growth geometry and impingement mechanisms.

In the following sections, microstructural paths obtained through this fully discrete formulation are presented and compared for different grain growth geometries, highlighting the implications of growth anisotropy and interface evolution on recrystallization kinetics.

3.3. Transformed volume fraction

Within the discrete simulation framework adopted in this work, X_r is obtained directly from the evolving voxelized microstructure. At each discrete simulation step τ, recrystallized and non-recrystallized regions are explicitly identified, allowing the temporal evolution of X_r to be tracked without invoking phenomenological kinetic laws or fitting procedures.

In all simulations, grain growth is governed by explicitly prescribed geometric parameters. Grain morphology is defined by the axial ratio K_a (see Section 2.2) and grain orientation is controlled by the angles Φ and θ, which define the alignment of the spheroidal growth axes relative to the Cartesian coordinate system. This parameterization enables a systematic assessment of the influence of grain shape and orientation on recrystallization kinetics.

The quantity X_r is evaluated, as defined in Section 3.2, as the ratio between the number of transformed cells and the total number of cells in the simulation domain. Expressed as a function of the discrete simulation time τ, the evolution of X_r reflects the combined effects of growth geometry and impingement behavior, which emerge naturally from the discrete growth process.

Figure 2 presents representative examples of the evolution of the number of transformed cells, N_{CT}, with the discrete simulation time τ for simulations performed in a cubic domain containing a single nucleus located at the domain center. Three growth geometries are considered: spherical growth, prolate spheroidal growth with axial ratio $K_a = 4$, and oblate spheroidal growth with axial ratio $K_a = 1/4$. In all cases, spheroidal grains are initially aligned with the base orientation ($\Phi = 0$, $\theta = 0$). The results highlight the initial growth regime prior to impingement with the

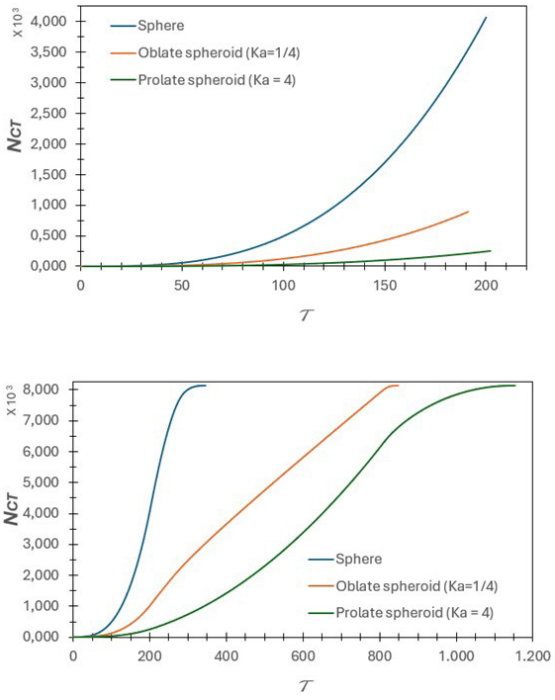

Figure 2. Evolution of the number of transformed cells N_{CT} as a function of discrete time τ for a single central nucleus in a cubic domain with 201^3 cells. The upper plot highlights the pre-impingement regime, while the lower plot shows the complete simulation.

domain boundaries, followed by the later stages leading to full domain occupation.

To evaluate recrystallization kinetics under more representative conditions, Figures 3 and 4 show the evolution of X_r as a function of τ for simulations performed in larger domains composed of 200^3 cells, with 1000 nuclei randomly distributed at the initial simulation step.

Figure 3 compares results obtained using classical CA with face-based neighborhood search, resulting in octahedral grain growth, and HCA with spherical grain growth. Despite identical nucleation densities and domain sizes, noticeable differences in the evolution of X_r are observed, indicating the influence of growth geometry and interface topology on transformation kinetics.

Figure 4 further explores the effect of growth anisotropy by considering prolate spheroidal grains with axial ratio $K_a = 4$. Two configurations are examined: a homogeneous orientation case, in which all grains share the same base orientation, and a heterogeneous orientation case, in which grains located in different regions of the domain grow according to distinct orientation parameters. The resulting $X_r(\tau)$ curves demonstrate that orientation-dependent growth leads to measurable variations in transformation kinetics, even under otherwise identical nucleation and domain conditions.

Overall, the results presented in this section demonstrate that the transformed volume fraction is strongly influenced by grain shape, growth anisotropy, and orientation. Because X_r is computed directly from the voxelized microstructure,

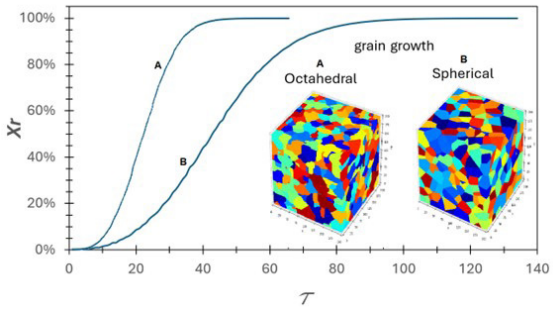

Figure 3. Evolution of the transformed volume fraction X_r as a function of discrete time τ in a 200^3 cell domain with 1000 randomly distributed nuclei. Classical cellular automata (CA) with octahedral grain growth (A – left plot) and hybrid cellular automata (HCA) with spherical grain growth (B – right plot).

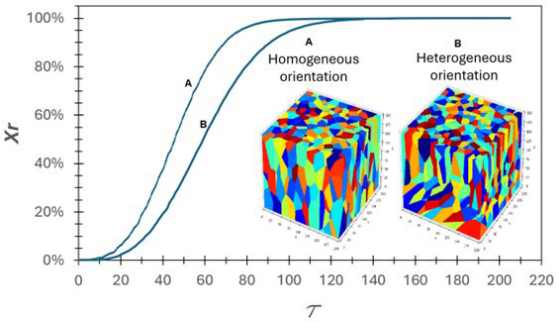

Figure 4. Evolution of the transformed volume fraction X_r as a function of discrete time τ in a 200^3 cell domain with 1000 randomly distributed nuclei and prolate spheroidal grains ($K_a = 4$). Homogeneous base orientation ($\Phi = 0$, $\theta = 0$) (A – left plot) and heterogeneous orientation, with $\Phi = 7\pi/12$ and $\theta = \pi/4$ for $Z < 100$ (B – right plot).

these effects are captured explicitly within the discrete framework, providing a consistent basis for the subsequent analysis of microstructural paths derived from fully discrete interfacial descriptors.

3.4. Fully discrete microstructural path

The fully discrete microstructural path is obtained by directly evaluating the evolution of S_{VRN} with the discrete simulation time τ, and subsequently relating this quantity to X_r . In contrast to hybrid formulations, no phenomenological expressions are employed; all relevant quantities are extracted directly from the voxelized microstructure.

At each simulation step, the three-dimensional matrix representing the material is scanned to identify interfacial voxels. A voxel is classified as interfacial if it belongs to a recrystallized grain and shares at least one face with a neighboring voxel that remains in the non-recrystallized state. Face adjacency is adopted because it provides a consistent and unambiguous definition of interfacial contact within a cubic voxel lattice.

Let $C_{RN}(\tau)$ denote the total number of voxels that simultaneously (i) belong to a recrystallized grain and (ii) are face-adjacent to at least one voxel in the non-recrystallized state at the discrete time τ . This quantity is obtained by scanning the entire simulation domain and counting only those recrystallized voxels whose six face-neighbors include at least one non-recrystallized voxel. In this way, only voxels located at recrystallized/non-recrystallized interfaces contribute to the interfacial area.

Once $C_{RN}(\tau)$ is determined, the discrete interfacial surface area, denoted as SF_{RN} , is computed as

$$SF_{RN}(\tau) = k_s r^2 C_{RN}(\tau) \tag{8}$$

where r is the linear resolution of the cubic voxels and k_s is a proportionality factor that corrects the face-counted discrete surface to its continuous-area equivalent. This correction accounts for geometric discretization effects inherent to voxel-based representations and is treated as a constant for the lattice employed in this work.

The corresponding interfacial surface area density is then obtained by normalizing the discrete surface area by the total simulation volume V_m :

$$S_{VRN}(\tau) = \frac{SF_{RN}(\tau)}{V_m} \tag{9}$$

By evaluating $S_{VRN}(\tau)$ and $X_r(\tau)$ at each simulation step, the microstructural path $S_{VRN}(X_r)$ is constructed entirely from discrete geometric information. This procedure captures the true evolution of interface topology during recrystallization, including the growth, impingement, and eventual disappearance of recrystallized/non-recrystallized interfaces as the transformation approaches completion.

For illustration, Figure 5 presents the evolution of SF_{RN} as a function of the discrete time τ for the simulations discussed in Section 3.3. Figures 6–9 subsequently show the corresponding microstructural paths, expressed as S_{VRN} versus X_r , for the same simulation conditions. These results demonstrate that the fully discrete formulation provides a consistent and physically transparent description of recrystallization kinetics, without reliance on phenomenological models such as Avrami or KJMA.

3.5. Practical relevance and validation of the fully discrete microstructural path

To complement the methodological developments presented in the previous sections and to assess their relevance for practical recrystallization phenomena in metals, a comparative application is presented using a well-documented experimental reference. The objective of this section is to evaluate whether the fully discrete formulation of the microstructural path, obtained exclusively from voxel-based geometric information, is capable of reproducing the characteristic features of recrystallization paths previously established through experimental observation and hybrid or phenomenological modeling approaches.

For this purpose, the classical experimental study conducted by Vandermeer and Rath (V&R)[28] is adopted as the primary reference. In that work, the recrystallization of high-purity iron was investigated over a temperature range from 450°C to 600°C, using a single crystal deformed by

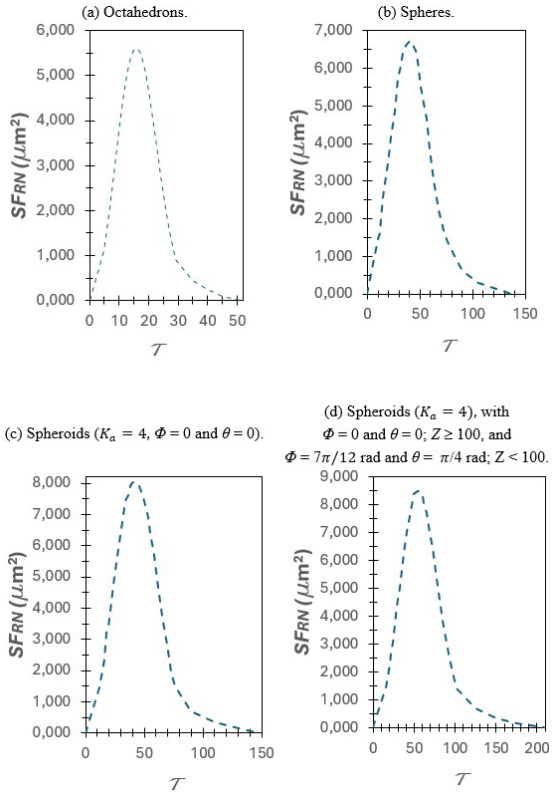

Figure 5. Evolution of the interfacial surface area between recrystallized and non-recrystallized regions, SF_{RN}, as a function of the discrete simulation time τ.

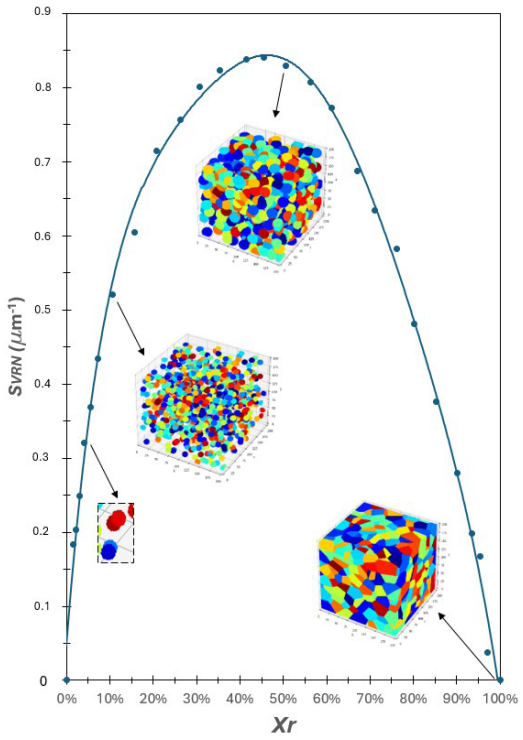

Figure 7. Microstructural path for spherical grain growth (1000 randomly distributed nuclei, 200^3 voxel domain).

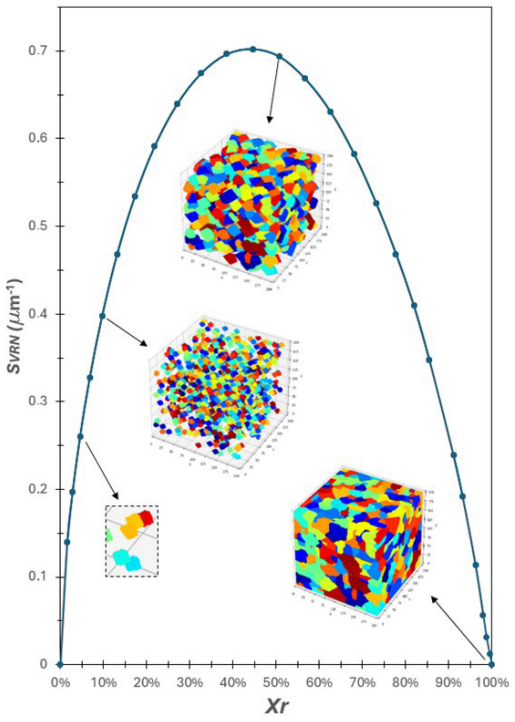

Figure 6. Microstructural path for octahedral grain growth (classical cellular automata, 1000 randomly distributed nuclei, 200^3 voxel domain).

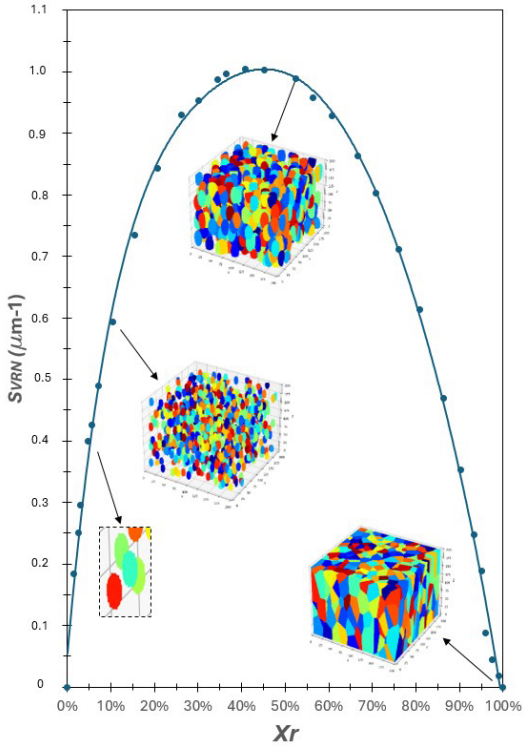

Figure 8. Microstructural path for spheroidal grain growth ($K_a = 4$, base orientation with $\Phi = 0$ and $\theta = 0$; 1000 randomly distributed nuclei, 200^3 voxel domain).

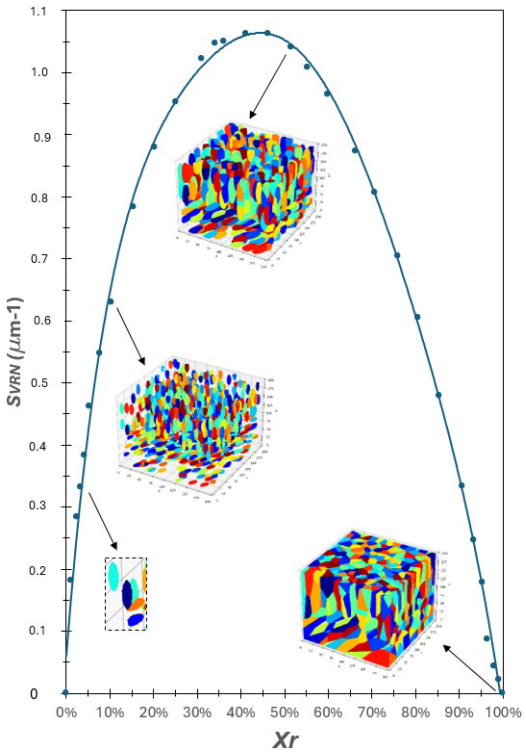

Figure 9. Microstructural path for spheroidal grain growth ($K_a = 4$) with spatially varying orientation: base orientation ($\Phi = 0$, $\theta = 0$, $Z \geq 100$) and rotated orientation ($\Phi = 7\pi/12$, $\theta = \pi/4$, $Z < 100$), with 1000 randomly distributed nuclei, 200^3 voxel domain.

approximately 70% cold rolling. In addition to reporting recrystallization kinetics, V&R provided a detailed experimental characterization of the microstructural path, expressed as the evolution of the interfacial surface area density between recrystallized and non-recrystallized regions as a function of the transformed volume fraction. This study has since become a benchmark for both experimental investigations and modeling approaches to recrystallization.

An additional and highly relevant reference is the independent computational analysis performed by Salazar, Assis, and Rios (SAR)[18], who revisited the V&R experiment using classical CA modeling. Their simulations were carried out in a cubic domain of 300^3 voxels, with 220 nuclei introduced simultaneously, corresponding to site-saturation nucleation. The nuclei were randomly distributed, resulting in a grain density of approximately 2.4×10^3 grains mm^{-3}, consistent with the experimental conditions. A voxel resolution of $r = 1.5$ mm was adopted. Grain growth occurred through face-based neighborhood rules, leading to octahedral grain shapes prior to impingement. Periodic boundary conditions were employed, and the KJMA formulation was used as a reference framework for interpreting and validating the computational results.

In the present work, simulations were intentionally performed under the same geometric and nucleation conditions adopted by SAR, namely the same domain size, number of nuclei, voxel resolution, and resulting grain density. This deliberate choice enables a direct and meaningful comparison between different modeling strategies. Two distinct growth formulations were investigated: (i) classical CA with face-based growth, producing octahedral grains, and (ii) HCA with spherical grain growth, which more closely reflects the morphology of recrystallized grains observed experimentally, particularly at early stages of recrystallization.

Despite this alignment in geometric and nucleation parameters, the modeling philosophy adopted here differs fundamentally from previous computational studies. All simulations in the present work were performed using non-periodic boundary conditions, and all grains were assumed to grow at identical velocities prior to impingement. Most importantly, the construction of the microstructural path relies exclusively on discrete quantities directly extracted from the evolving voxelized microstructure, following the procedures detailed in Sections 3.3 and 3.4. No phenomenological kinetic equations, such as the Avrami or KJMA formulations, were employed at any stage of the analysis. Likewise, no empirical correction factors, fitting parameters, or experiment-specific adjustments were introduced to guide, calibrate, or constrain the results.

For illustration, Figure 10 presents representative images of the simulations performed using HCA with spherical grain growth, shown at approximately 5% transformed volume fraction and after complete recrystallization, for a mean grain density of 2400 grains mm^{-3}.

Figure 11 presents the central result of this section: a direct comparison between the microstructural path obtained in the present work and schematic representations of the paths reported in the literature, namely the experimental path originally measured by V&R, as subsequently adapted into a continuous representation by SAR, and the corresponding computational results reported by SAR. The comparison shows that the fully discrete microstructural path reproduces the characteristic non-monotonic evolution observed in previous studies, with an initial increase in interfacial surface area density, followed by a well-defined maximum and a subsequent decrease as impingement between recrystallized grains becomes dominant. In addition to capturing the qualitative shape of the path, the calculated values are also in close quantitative agreement with the corresponding results reported by SAR and derived from the experimental data of V&R.

The similarity in the overall shape and relative position of the curves is particularly noteworthy given the complete

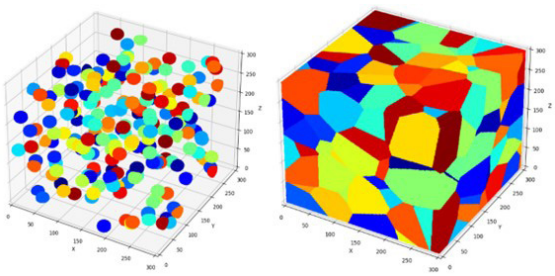

Figure 10. Simulation snapshots obtained using hybrid cellular automata (HCA) with spherical grain growth and an average grain density of 2400 grains mm^{-3}, shown at approximately 5% transformed volume fraction and at complete recrystallization.

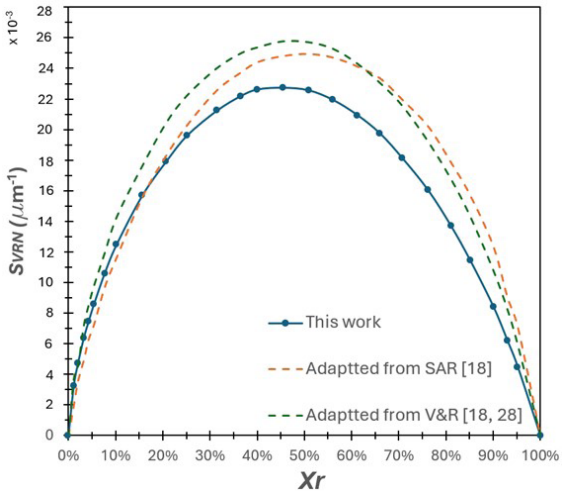

Figure 11. Microstructural path obtained in the present work, compared with schematic representations of the paths reported by SAR[18] and derived from the experimental results of V&R[28], as interpreted by SAR.

absence of phenomenological support or calibration. In contrast to hybrid approaches, where discrete simulation outputs are commonly interpreted or constrained using analytical expressions derived from continuous theories, the present results emerge solely from the geometric evolution of the voxelized microstructure. To the authors' knowledge, this work provides one of the first demonstrations in the literature that a microstructural path can be obtained entirely through a fully discrete formulation, without recourse to phenomenological kinetic equations or ad hoc adjustment factors, while still yielding trends and magnitudes consistent with experimentally validated benchmarks.

It should be emphasized that, under the assumptions adopted here, real time and temperature do not explicitly enter the simulations. All nuclei are introduced simultaneously, and all grains grow at identical rates prior to impingement. Consequently, the absolute transformation time and thermal history do not influence the resulting microstructural path. While time and temperature are fundamental parameters in practical recrystallization processes, within the present framework they act as external variables that can be mapped onto the discrete evolution once the geometric description has been established. The incorporation of thermally activated kinetics, heterogeneous growth rates, and time-dependent nucleation therefore represents a natural and important direction for future extensions of the proposed methodology.

Overall, the results presented in this section demonstrate that a fully discrete, geometry-based description of the microstructural path is not only theoretically consistent but also practically meaningful, in line with microstructural path modeling studies that successfully describe recrystallization kinetics in industrial alloys by incorporating anisotropic growth and spatially non-uniform nucleation conditions[29]. The agreement with classical experimental and computational references, achieved without invoking phenomenological kinetic models, underscores the robustness of the proposed approach and highlights its potential as a foundation for future developments in computational recrystallization modeling.

4. Conclusions

This work presented a fully discrete formulation for the analysis of recrystallization microstructures based on three-dimensional hybrid cellular automata simulations. By extracting all relevant descriptors directly from the evolving voxelized microstructure, the proposed approach enables the construction of microstructural paths without reliance on phenomenological kinetic equations or auxiliary analytical models, such as the Kolmogorov–Johnson–Mehl–Avrami formulation.

The transformed volume fraction and the interfacial surface area density between recrystallized and non-recrystallized regions were obtained exclusively from discrete geometric information. This allowed the microstructural path to be evaluated as a purely geometry-driven descriptor, capturing the evolution of interfaces throughout nucleation, growth, impingement, and completion of recrystallization. The resulting framework is transparent and reproducible, with each quantity having a direct geometric and physical interpretation.

Comparative analyses were performed using different growth geometries, including classical face-based cellular automata growth and hybrid cellular automata formulations with spherical and spheroidal grains. The results demonstrate that grain morphology and growth anisotropy exert a measurable influence on the shape and evolution of the microstructural path, emphasizing the importance of geometric assumptions in recrystallization modeling and in the interpretation of microstructural path curves.

The practical relevance of the fully discrete formulation was assessed through comparison with established experimental and computational references reported in the literature. Despite the absence of fitting parameters or experiment-specific corrections, the discrete microstructural paths obtained in this work reproduce the characteristic non-monotonic behavior of microstructural paths observed in recrystallization of pure metals. This agreement indicates that the essential features of microstructural path evolution can be captured through discrete geometric descriptors alone, without invoking analytical kinetic laws.

Within the scope of the modeling assumptions adopted in this study, namely site-saturation nucleation, uniform growth rates prior to impingement, and non-periodic boundary conditions, the proposed methodology provides a consistent alternative to hybrid computational–phenomenological approaches. Rather than replacing established kinetic models, the fully discrete formulation offers an independent and complementary perspective, particularly well suited for investigations focused on microstructural geometry, interface topology, and the intrinsic evolution of interfacial area.

Although real time and temperature were not explicitly incorporated into the simulations, the results suggest that the microstructural path itself is fundamentally governed by geometric evolution. The explicit coupling of the present framework with thermally activated kinetics, heterogeneous growth rates, and time-dependent nucleation laws represents a natural and important direction for future developments, with

the potential to further strengthen the connection between discrete modeling and experimental recrystallization kinetics.

Overall, this study demonstrates that a fully discrete, geometry-based description of recrystallization microstructural paths is both feasible and physically meaningful. By minimizing modeling assumptions and avoiding phenomenological constraints, the proposed approach contributes to a clearer understanding of the relationship between microstructural geometry and transformation behavior, and provides a robust foundation for future advances in computational materials science.

5. Data Availability

All the data supporting the results of this study are presented within the article itself.

6. References

1. Rios PR, Padilha AF. Microstructural path of recrystallization in a commercial Al–Mn–Fe–Si (AA3003) alloy. Mater Res. 2003;6(4):605-13. https://doi.org/10.1590/S1516-14392003000400030.
2. Rios PR, Padilha AF. Transformações de fase. São Paulo: Artliber; 2007.
3. Vandermeer RA. Microstructural descriptors and the effects of nuclei clustering on recrystallization path kinetics. Acta Mater. 2005;53(5):1449-57. https://doi.org/10.1016/j.actamat.2004.10.054.
4. Humphreys FJ, Hatherly M. Recrystallization and related annealing phenomena. 2nd ed. Oxford: Elsevier; 2004. https://doi.org/10.1016/B978-0-08-044164-1.X5000-2.
5. Godiksen RB, Rios PR, Vandermeer RA, Schmidt S, Jensen DJ. Three-dimensional geometric simulations of random anisotropic growth during transformation phenomena. Scr Mater. 2008;58(4):279-82. https://doi.org/10.1016/j.scriptamat.2007.10.003.
6. Villa E, Rios PR. On volume and surface densities of dynamical germ–grain models with ellipsoidal growth. Stochastic Anal Appl. 2020;38(6):1134-55. https://doi.org/10.1080/07362994.2020.1773276.
7. Vandermeer RA, Jensen DJ. Microstructural path modeling of primary recrystallization. J Phys Conf Ser. 2023;2635(1):012027. https://doi.org/10.1088/1742-6596/2635/1/012027.
8. Janssens KGF. An introductory review of cellular automata modeling of moving grain boundaries in polycrystalline materials. Math Comput Simul. 2010;80(7):1361-81. https://doi.org/10.1016/j.matcom.2009.02.011.
9. Hesselbarth HW, Göbel IR. Simulation of recrystallization by cellular automata. Acta Metall Mater. 1991;39(9):2135-43. https://doi.org/10.1016/0956-7151(91)90183-2.
10. Hallberg H. Approaches to modeling of recrystallization. Metals. 2011;1(1):16-48. https://doi.org/10.3390/met1010016.
11. Hallberg H, Wallin M, Ristinmaa M. Simulation of discontinuous dynamic recrystallization in pure Cu using a probabilistic cellular automaton. Comput Mater Sci. 2010;49(1):25-34. https://doi.org/10.1016/j.commatsci.2010.04.012.
12. Chen F, Zhu H, Zhang H, Cui Z. Mesoscale modeling of dynamic recrystallization: multilevel cellular automaton simulation framework. Metall Mater Trans, A Phys Metall Mater Sci. 2020;51(3):1286-303. https://doi.org/10.1007/s11661-019-05620-3.
13. Łach Ł. Modeling of microstructure evolution during deformation processes by cellular automata. Materials. 2021;14(6):1377. https://doi.org/10.3390/ma14061377.
14. Perzyński K. The effect of model size and boundary conditions on the representativeness of digital material representation simulations of ferritic-pearlitic sample compression. Comput Methods Mater Sci. 2022;22(2):59-66. https://doi.org/10.7494/cmms.2022.2.0780.
15. Braga HC, Silva SN. Study of recrystallization in metals through equiaxial growth using hybrid cellular automata. Mater Res. 2025;28:e20250204. https://doi.org/10.1590/1980-5373-mr-2025-0204.
16. Braga HC, Silva SND, Corrêa ECS. Modeling and simulation of recrystallization in metals with spheroidal grain structures using hybrid cellular automata. Materia. 2026;31:e20250758. https://doi.org/10.1590/1517-7076-rmat-2025-0758.
17. Hull R, Keblinski P, Lewis D, Maniatty A, Meunier V, Oberai AA, et al. Stochasticity in materials structure, properties, and processing – a review. Appl Phys Rev. 2018;5(1):011302. https://doi.org/10.1063/1.4998144.
18. Salazar TC, Assis WLS, Rios PR. Simulation of recrystallization in iron single crystals. Mater Res. 2008;11(1):109-15. https://doi.org/10.1590/S1516-14392008000100021.
19. Liu X, Zhu J, He Y, Jia H, Lim B, Fang G. State-of-the-art review of dynamic recrystallization simulation. Metals. 2024;14(11):1230. https://doi.org/10.3390/met14111230.
20. Umemoto M, Guo ZH, Tamura I. Effect of cooling rate on ferrite grain size. Mater Sci Technol. 1987;3(4):249-55. https://doi.org/10.1179/mst.1987.3.4.249.
21. Alves ALM, Assis WLS, Rios PR. Quantitative metallographic parameters for multiphase microstructures. Mater Res. 2023;26:e20220476. https://doi.org/10.1590/1980-5373-mr-2022-0476.
22. Rhines FN, Patterson BR. Effect of prior cold work on grain growth of recrystallized aluminum. Metall Trans, A, Phys Metall Mater Sci. 1982;13(6):985-93. https://doi.org/10.1007/BF02643395.
23. Takayama Y, Furushiro N, Tozawa T, Kato H, Hori S. A significant method for estimation of the grain size of polycrystalline materials. Mater Trans JIM. 1991;32(3):214-21. https://doi.org/10.2320/matertrans1989.32.214.
24. Lindblad J. Surface area estimation of digitized 3D objects using weighted local configurations. Image Vis Comput. 2005;23(2):111-22. https://doi.org/10.1016/j.imavis.2004.06.012.
25. Sánchez-Cruz H, Sossa-Azuela H, Braumann U-D, Bribiesca E. The Euler–Poincaré formula through contact surfaces of voxelized objects. J Appl Res Technol. 2013;11(1):65-78. https://doi.org/10.1016/S1665-6423(13)71515-3.
26. Oliveira VT, Oliveira LP, Rios PR, Castro JA. Desenvolvimento de um código em 3D para simular a recristalização pelo método do autômato celular. Tecnol Metal Mater Min. 2006;2(4):34-9. https://doi.org/10.4322/tmm.00204007.
27. Vandermeer RA, Jensen DJ. Quantification of microstructural evolution and texture development during recrystallization. Texture Stress Microstruct. 1996;26(1):263-79. https://doi.org/10.1155/TSM.26-27.263.
28. Vandermeer RA, Rath BB. Modeling recrystallization kinetics in a deformed iron single crystal. Metall Trans, A, Phys Metall Mater Sci. 1989;20(3):391-401. https://doi.org/10.1007/BF02653918.
29. Vandermeer R, Lei X, Knipschildt-Okkels E, Lin F, Sanders R, Jensen D. Advanced microstructural path modeling of primary recrystallization in aluminum alloys AA5182 and AA5657. MetalMat. 2024;1(1):e15. https://doi.org/10.1002/metm.15.